Wadi Alshatti University Journal of
Pure and Applied Sciences

مجلة جامعة وادي الشاطئ
للعلوم البحتة والتطبيقية

Volume 4, No. 2, July-Decemer 2026 Online ISSN: 3006-0877 المجلد 4، الاصدار 2، يوليو- ديسمبر 2026

RESEARCH ARTICLE POWER MECHANICAL ENGINEERNG

Optimization Study of Converting the Derna Steam Power Plant to a Combined Gas/Steam Cycle

Ahmed A. Otman[1,*], Shahat M. Alfkhakhri[1], Fouzi M. Mossa[2], Rabae H. Mustafa[1], Tarek A. Hamad[3], Abdul Hakim Awami[4], Yasser F. Nassar[5], Ibrahim K. Mangir[6]

[1] Department of Mechanical Engineering, College of Technical Sciences, Derna, Libya
[2] Department of Mechanical Engineering, Omar Al-Mukhtar University, Libya
[3] Department of Sustainable and Renewable Energy Engineering, Omar Al-Mukhtar University, Libya
[4] Department of Electrical Engineering, College of Technical Sciences, Derna, Libya
[5] Department of Mechanical and Renewable Energy Engineering, Wadi Alshatti University, Brack, Libya
[6] Higher Institute of Sciences and Technology, Tamezawa, Brack, Libya

ARTICLE HISTORY
Received 11 April 2026
Revised 24 April 2026
Accepted 16 June 2026
Online 27 June 2026

KEYWORDS
Combined Gas/Steam Cycle;
Steam Power Plant;
Efficiency;
Derna;
Libya.

ABSTRACT

Research efforts have switched to increasing the efficiency of systems that convert thermal energy into mechanical labor due to the rise in the cost of oil and fuel gas over the past 20 years and the risks of environmental contamination.. Combined gas/steam power plants (CGSPP) are becoming more widespread due to their excellent thermal efficiency, higher capacity, and low environmental impact. The current research focuses on the theoretical analysis of CGSPP, which uses a single-pressure heat recovery boiler without supplemental fire. A computer program for the studied combined cycle based on the burning of 1 kmoles of natural gas in the combustor of the gas turbine is built utilizing the conservation equations for mass and energy, as well as combustion calculations. Each component of the combined cycle is assigned a unique subprogram using Engineering Equation Solver (EES). The results reveal that the combined cycle's maximum efficiency may be obtained at around 47.24 ٪ as long as the boiler pressure remains constant. Since improved combined-cycle efficiency is the goal, modest compressor pressure ratios must be used. At a high compressor pressure ratio, the boiler pressure must be reduced to maintain a positive temperature differential at the pinch point. To minimize a loss in combined cycle efficiency at high compressor pressure ratios, we propose using a dual-pressure boiler.

دراسة تحسين تحويل محطة درنة لتوليد الطاقة البخارية إلى دورة غاز/بخار مشتركة

احمد عثمان[1،*]، شحات الفخاخري[1]، فوزي الحاسي[2]، ربيع الشلوي[1]، طارق الترهوني[3] عبدالحكيم العوامي[4]، ياسر نصار[5]، ابراهيم المعنقر[6]

الكلمات المفتاحية
محطة البخارية الغازية المشتركة
محطة توليد الطاقة البخارية
الكفاءة
درنة
ليبيا

الملخص

اتجهت جهود البحث نحو زيادة كفاءة الأنظمة التي تحول الطاقة الحرارية إلى طاقة ميكانيكية، وذلك نتيجة لارتفاع تكلفة النفط والغاز خلال العشرين عامًا الماضية، فضلًا عن مخاطر التلوث البيئي. وتنتشر محطات توليد الطاقة المركبة بالغاز والبخار (CGSPP) على نطاق أوسع نظرًا لكفاءتها الحرارية الممتازة، وقدرتها الإنتاجية العالية، وانخفاض أثرها البيئي. يركز البحث الحالي على التحليل النظري لمحطات CGSPP التي تستخدم غلاية استعادة حرارة أحادية الضغط دون استخدام نار إضافية. تم بناء برنامج حاسوبي للدورة المركبة المدروسة، استنادًا إلى حرق 1 كيلومول من الغاز الطبيعي في غرفة احتراق التوربين الغازي، وذلك باستخدام معادلات حفظ الكتلة والطاقة، بالإضافة إلى حسابات الاحتراق. تم تخصيص برنامج فرعي فريد لكل مكون من مكونات الدورة المركبة باستخدام برنامج حل المعادلات الهندسية (EES). تُظهر النتائج أن أقصى كفاءة للدورة المركبة يمكن الحصول عليها عند حوالي 47.24 درجة مئوية، طالما ظل ضغط الغلاية ثابتًا. ولأن الهدف هو تحسين كفاءة الدورة المركبة، يجب استخدام نسب ضغط معتدلة للضاغط. عند نسبة ضغط عالية للضاغط، يجب خفض ضغط الغلاية للحفاظ على فرق درجة حرارة موجب عند نقطة الاختناق. ولتقليل فقدان كفاءة الدورة المركبة عند نسب ضغط عالية للضاغط، نقترح استخدام غلاية ثنائية الضغط.

Introduction

Energy (in all its forms) is the major driving force behind human society's growth. According to statistics, fossil fuels account for approximately 80% of primary energy utilized globally [1]. It is expected that the amount of electrical energy consumed would double over the next 20 years, driven by population increase and technological improvement [2]. By the end of 2025, worldwide electricity generation will have reached roughly 30,850 TWh, with fossil fuels (coal, gas, and oil) accounting for 58%, renewables (hydro, wind, solar, bioenergy, and geothermal) accounting for 32%, and nuclear accounting for 10%. Global power consumption is rapidly increasing, with a predicted 4.5% rise by 2025;

*Corresponding author
https://doi.org/10.63318/waujpasv4i2_07

ensuring that future generations have enough energy is a big problem for any country attempting to expand sustainably [3]. On the other side, this will result in greater environmental degradation and a dramatic shift in the ecosystem, leading to a slew of environmental issues such as global warming, climate change, disease spread, starvation, drought, and desertification The situation is similar in Libya, where rising population and economic growth have increased energy consumption, necessitating more electric power plants and distribution networks. Figure 1 depicts the growing demand for power in Libya. In Libya, electricity production in 2024 reached approximately 33,980 gigawatt-hours. Libya relies almost entirely on fossil fuels (natural gas and liquid fuels) for electricity generation, with estimates indicating a dependence rate exceeding 99% (Countryeconomy.com, 2025). Steam power plants contributed 13.7%, gas-fired power plants 59.3%, and combined-cycle power plants 26.1%, while renewable energy sources accounted for less than 1% of the energy mix. Libya generates electricity from fossil fuels as follows: heavy oil 19.4%, light oil 35.3%, natural gas 38.2%, and crude oil 7.1% [5]. The emissions associated with electricity generation in Libya are estimated at approximately 32.871 million tons of CO_2 per year [6,7]. By 2025, Libya hopes to enhance electricity capacity by adding 10% of total capacity using renewable sources. However, due to the country's security situation, this plan was stopped in 2011. Following the country's relative security in 2020, the state revised its strategic plan, which it revealed during the COP27 summit held in Sharm El-Sheikh, Egypt, from 8-14 November 2022, with the goal of increasing the contribution of renewable energy in the mix of electric power generation in Libya to 30% by 2030 and 50% by 2050. This will be accomplished by the application of concentrated solar, solar photovoltaic, and wind energy [8-10].

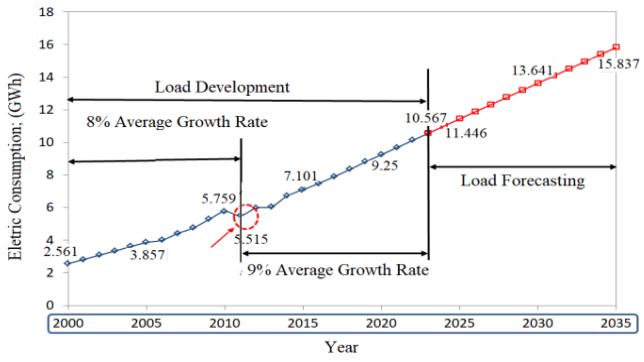

Figure 1: Development of rising demand for electricity in Libya

Sustainable energy production necessitates meticulous actions toward efficiency improvement (resource management) and produces environmentally benign energies. Thermal power plants are the most prevalent in various power generation locations across the world. These sectors are being driven to change their technology, adopt more environmentally friendly practices, and implement high-efficiency cycles. As a result, multi-objective optimization of a combined cycle power plant in terms of cost, efficiency, and environmental impact is one step closer to resolving this issue. A power plant is an important part of the energy production process. Among many types of power plants, CCPPs have received a lot of attention because they are more desirable in the power production area than individual steam or gas turbine power plants and have a lower environmental effect [11–14]. Under these conditions, improving the thermodynamic efficiency of existing thermal power plants is both an economic demand to reduce fuel consumption and an environmental requirement to limit emissions [15].To maximize the efficiency, cost effectiveness, and environmental impact of such plants, it is vital to know the locations, kinds, and magnitudes of genuine inefficiencies (irreversibilities) beforehand. Various power supply system's exist and are described in literature, including nuclear energy, wind energy, water energy, steam turbines (ST), and gas turbines (GT). In this aspect, steam serves as the primary source of power for a variety of operations such as heating, chemical reactions, and power generation. As fuel costs continue to climb, researchers and development engineers must create innovative ways for maximizing energy supply and generation, enhancing efficiency, reducing fuel consumption, and optimizing power plant costs. Despite advances in alternative energy technologies, the bulk of the world's electricity is still generated in thermal power plants using burning boilers and steam turbines. Recently, combined cycle gas turbines (CCGT) have been regarded as more efficient for power generation [16]. CCGT typically provides the maximum efficiency for power generation [17]. Thermal approaches continue to dominate the technological mix in the enhanced oil recovery (EOR) sector, indicating continued steam-intensive recovery activities. [18].A CCGT's thermal efficiency can surpass 60%, depending on the circumstances and the design of the cycle's components [19]. The combined cycle gas turbine (CCGT) is made up of two major components: the gas turbine [20] and the steam turbine [21]. A gas turbine (GT) is an internal combustion engine that converts the chemical energy of fuel into mechanical energy by using gaseous energy from the air. The steam turbine is a device that captures thermal energy from pressured steam and converts it into mechanical work. The thermodynamic integration of these two systems to act as a single system is known as "cogeneration," which refers to the simultaneous generation of work (shaft power) and heat (steam). Cogeneration systems may operate at high capacity and efficiency almost all year. Cogeneration systems are 30% more energy efficient than standard energy systems [22]. Thermodynamically, combining two thermal cycles in a single power plant increases efficiency and conserves energy [23]. GT exhaust temperatures may vary from 500 to 600oC [24]. The combination of cycles with different working medium is quite fascinating since their benefits can compliment one another. When two cycles are combined, the cycle with the greater temperature is typically referred to as the "topping cycle". The waste heat produced is then employed in a second process known as the "bottoming cycle" [25], which runs at a lower temperature level. It consequently makes technical sense to take use of the gas-turbine cycle's highly desired properties at high temperatures and use the high-temperature exhaust gases as an energy source for the steam power cycle [26]. The most frequently recognized combination for commercial power generation and marine propulsion applications is a gas topping cycle followed by a steam bottoming cycle [27]. Along with its widespread and successful use in land-based power plants, the combined gas and steam turbine (COGAS) idea is being expanded to provide an alternative kind of power plant for ships [28]. COGAS is not to be confused with combined steam and gas power plants, which use oil-fired boilers for steam turbine propulsion during normal sailing and add gas turbines for high speed and faster response/reaction times. The COGAS plant uses heat from the gas turbine's exhaust

gas to heat water via a series of tubes in a heat exchanger under high pressure, producing superheated steam. In this plant, the network is a mix of work done in gas and steam turbines, all from a single source of heat supply [29]. These systems' flexibility makes them suitable for utility power generation, industrial cogeneration, and ship propulsion applications, where their efficiency can surpass 60% [30]. Modeling and simulation of coupled cycles has long been an effective approach for improving their performance. However, the requirement to construct accurate and dependable COGAS models for various purposes and applications has provided tremendous motivation for academics to continue working in this exciting field [31]. According to the International Energy Agency (IEA), global electricity output is predicted to rise faster than any other source of energy, with demand for power potentially exceeding 2.2% each year between 2008 and 2035 [32].As a result, there is a rising requirement for additional resources and innovative technology to sustain expansion and ensure universal access to power services. In reality, fossil fuel power plants generate more than 65% of the world's electrical energy [33,34]. The worldwide energy supply sector agrees that Combined Cycle Gas Turbine facilities (CCGT) are the preferred production technology for private investors. CCGT represent the link between fossil fuel-based energy production technologies and the transition to renewable and innovative sources of energy. As a result, energy production will continue to rely on fossil fuels for the foreseeable future, and combined cycle plants are expected to see significant development in the coming years. In recent years, there has been an increased interest in the combined cycle gas turbine (CCGT), particularly in nations with abundant natural gas supplies [35]. Furthermore, employing natural gas rather of fossil fuels can result in significant efficiency gains [36]. The technological advancement of CCGT plants has occurred in stages, paralleling the development of the GT and steam cycles. These advantages are becoming increasingly essential in today's climate, where operational standards Other environmental regulations are becoming more rigorous. Furthermore, because of their reduced environmental effect, CCGT facilities take up less area than similar coal or nuclear reactors and have less site limitations. Furthermore, CCGT plants have minimal operating and maintenance expenses because to high-quality technology that allows for quick component inspection. The installation of CCGT is likely to rise even more rapidly in the next years, as new environmental criteria are implemented. As the power system evolves, modeling and simulation issues arise. Building a new engine model is time consuming and expensive in the traditional way, however a successful simulation model may be built without the requirement for prototypes in the early phases of design. Modeling is so more than just a mathematical workout; it also requires a thorough grasp of the system and its operation. However, modeling is considerably more difficult since judgments must be made about which occurrences and dynamics to ignore and which to mimic. As a result, simplified mathematical models of CCGTs are required to examine power system stability, define optimal operating strategies, and build contingency plans for system disruptions. There have been several research [37-39] published in this topic on gas turbine models. Several literature reviews [40,41] demonstrated that the use of simplified models can be a viable choice for representing the dynamic behavior of mixed cycle systems for various applications. However, dynamic simulation is an essential practice when the systems are operating at the process's limitations. This need complicated models that are as near as feasible to the real system. As a result, various studies have given mathematical models for thermal power under a variety of disturbance situations. These simulation models gave a thorough investigation of the power system's stability. Dynamic modeling enables investigations into the transient behavior of the complete thermal power plant and its associated control mechanisms. As a result, significant efforts have been made to better understand CCGT dynamics and build appropriate control systems, and there is tremendous desire to improve power plant performance [42, 43]. Remarkable research has been conducted on modeling and simulating systems, and a range of analytical and experimental models have been constructed thus far to gain a thorough grasp of the nonlinear behavior and dynamics of these complex systems. The information obtained from the mathematical model's simulation is extensively utilized to examine potential future advances and improvements. Advanced control systems, new simulators, and precise simulation models that represent the whole functioning of CCGT plants are extremely important and required. Converting the Derna steam power plant into a mixed gas/steam power plant with a single-stage heat recovery boiler is the aim of this research. The combined plant's performance will be evaluated in connection with gas cycle features (gas turbine inlet temperature and gas cycle pressure ratio). The molar composition, molecular weight, and calorific value of the fuel—natural gas—as provided by the National Oil Corporation (Libyan Petroleum Institute) are shown in Table 1. The information used in this study is shown in Table 2.

Methodology

An air compressor, a combustion chamber, and a gas turbine make up the basic open gas turbine cycle that is employed in this work as a combined gas/steam cycle. The components of the steam turbine cycle are identical to those of the Derna steam power plant; however, a single-stage heat recovery boiler that uses the flue gases leaving the gas turbine to generate steam takes the place of the boiler and burner. The other parts of the steam power plant in Derna are still in place. A four-stage expansion steam turbine, a condenser, pumps, a low-pressure superheater, an open deaerator, and a high-pressure superheater comprise the Derna steam power plant .The economizer, boiler or evaporator, and superheater are the three parts of the heat recovery boiler. The exhaust gases from the heat recovery boiler are released into the atmosphere through a chimney, and an energy generator is powered by both the gas and steam turbines. The combined gas/steam cycle design is shown in Figure 2, while the temperature-entropy graphs for the gas and steam plants are shown in Figure 3. Every component of a combined gas/steam power plant needs to go through a thermodynamic study in order to examine its performance. The following assumptions are made in order to conduct this thermodynamic analysis [44-46].

1. The specific heat of air and combustion gases varies with temperature.
2. Fixed values of atmospheric pressure, air temperature, and relative humidity (1 bar, 25°C, 70%) are used, ignoring changes in atmospheric conditions.
3. Assumed values for gas turbine, steam turbine, compressor, breakout chamber combustion efficiency, pump, mechanical, and generator efficiencies.

4. Neglect pressure losses in combustion chambers, heat recovery boilers, condensers, and pipelines.

$$p_{(O_2+N_2)} = p_{at} - p_v \quad (3)$$

5. The impact of pump operation is considered
6. The steam cycle characteristics will be the same as the Derna steam plant, with flue gases at 125°C.
7. The minimum temperature differential at the pinch point will be set at 15°C.

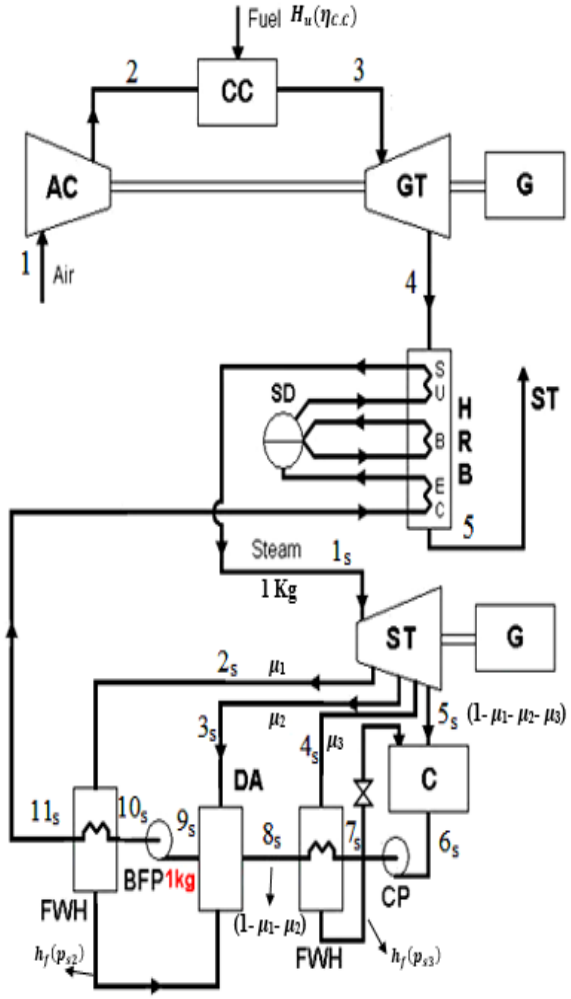

Figure 2: Schematic illustration of the combined gas and steam power plant

Gas turbine unit calculations

The gas-fired power plant uses the Brayton gas cycle, in which the compressor compression and turbine expansion are irreversible adiabatic processes. The gas-fired power plant calculations require the pressure ratio of the compressor π_C and the temperature of the combustion gases departing the combustion chamber and entering the turbine T_3.

Compression procedure in the compressor

The mole fraction of the components of humid atmospheric air, which include oxygen, nitrogen, and water vapor, is calculated as follows [44-46]:

The partial pressure of water vapor present in humid air is calculated from the relative humidity of the air (ϕ):

$$\emptyset = \frac{p_v}{p_s(T_1)} \quad (1)$$

$$p_v = \emptyset p_s(T_1) \quad (2)$$

Where:

p_v: partial pressure of water vapor present in humid air.

p_s: pressure at atmospheric air temperature.

$\emptyset$: relative humidity.

The pressure of dry air, which consists of (oxygen +nitrogen), is calculated from the atmospheric pressure (total

Where: $p_{at:}$ is the atmospheric air pressure.

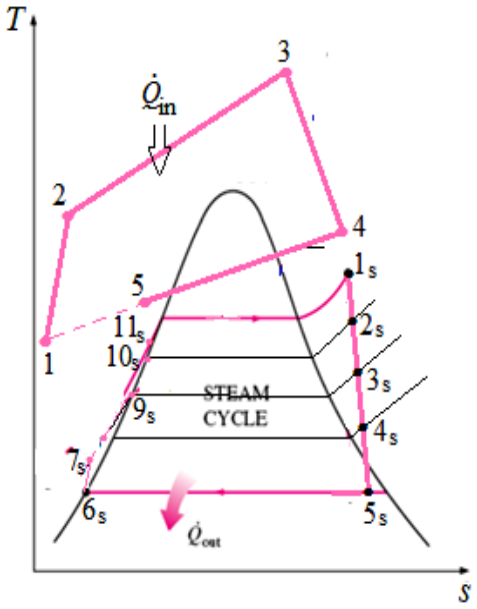

Figure 3: Temperature - Entropy of the Combined Station

Since the molar composition of dry air is 21% oxygen and 79% nitrogen, the partial pressure of both oxygen and nitrogen in humid atmospheric air is calculated as follows:

$$p_{O_2} = 0.21 \times p_{(O_2+N_2)} \quad (4)$$

$$p_{N_2} = 0.79 \times p_{(O_2+N_2)} \quad (5)$$

The mole fraction of oxygen, nitrogen, and water vapor in humid air is calculated as follows:

$$(n_{O_2})_{air} = \frac{p_{O_2}}{p_{atm}} \quad (6)$$

$$(n_{N_2})_{air} = \frac{p_{N_2}}{p_{atm}} \quad (7)$$

$$(n_{H_2+O})_{air} = \frac{p_v}{p_{atm}} \quad (8)$$

Where:

p_{O_2} is the partial pressure of oxygen in humid atmospheric air.

p_{N_2} is the partial pressure of nitrogen in humid atmospheric air.

Referring to Figure (2), we see that the humid air from the outside atmosphere enters the compressor at condition 1, where it increases in pressure and temperature before exiting at condition 2. The temperature of the air leaving the compressor is estimated using the compressor's isotropic efficiency as follows:

$$T_{2s} = T_1 \pi_C^{(\gamma-1)/\gamma}$$

$$T_2 = T_1 + (T_{2s} - T_1)/\eta_C \quad (9)$$

Where:

T_1: is the air temperature in (K),

π_C: is the compressor pressure ratio,

T_{2s}: is the temperature after isentropic compression (K),

γ: is the isentropic exponent of air (γ = $\widetilde{C}_{Pa}/\widetilde{C}_{va}$)
η_C: is the isentropic efficiency of the compressor.
$\widetilde{C}_{Pa}$ is the specific heat of air at constant pressure (kJ/(kmol.K))
$\widetilde{C}_{va}$ is the specific heat of air at constant volume (kJ/(kmol.K))
The work required by the compressor per kilomole of air is calculated from the following equation:

$$w_C = \frac{\tilde{C}_{Pa}(T_{2s} - T_1)}{\eta_{mC}} \; ; \; kJ/kmol \qquad (10)$$

Where:
η_{mC} is the compressor's mechanical efficiency
The process of combustion within the combustion chamber. The most important thermodynamic process in mixed gas/steam power plants is burning. The energy needed to produce electricity in the gas power plant is produced by burning fuel in the combustion chamber. This energy is then transferred to the steam power plant through a heat recovery boiler. The molar analysis of natural gas, the fuel used in this study, is shown in Table 1). The compressor delivers oxygen into the combustion chamber, which is necessary for the combustion process to be completed. The bare minimum of air required for the complete combustion of natural gas components is known as the theoretical air quantity. The theoretical air quantity. The following chemical combustion formulae for natural gas components are used to calculate the theoretical air quantity [44-46].

$$\begin{gathered} n_{CH_4}CH_4 + 2n_{CH_4}(O_2 + 3.76N_2) \rightarrow \\ n_{CH_4}CO_2 + 2n_{CH_4}H_2O + 7.52n_{CH_4}N_2 \\ n_{C_2H_6}C_2H_6 + 3.5n_{C_2H_6}(O_2 + 3.76N_2) \rightarrow \\ 2n_{C_2H_6}CO_2 + 3n_{C_2H_6}H_2O + 13.16n_{C_2H_6}N_2 \\ n_{C_3H_8}C_3H_8 + 5n_{C_3H_8}(O_2 + 3.76N_2) \rightarrow \\ 3n_{C_3H_8}CO_2 + 4n_{C_3H_8}H_2O + 18.8n_{C_3H_8}N_2 \\ n_{C_4H_{10}}C_4H_{10} + 6.5C_4H_{10}(O_2 + 3.76N_2) \rightarrow \\ 4n_{C_4H_{10}}CO_2 + 5n_{C_4H_{10}}H_2O + 24.44n_{C_4H_{10}}N_2 \\ n_{C_5H_{12}}C_5H_{12} + 8C_5H_{12}(O_2 + 3.76N_2) \rightarrow \\ 5n_{C_5H_{12}}CO_2 + 6n_{C_5H_{12}}H_2O + 30.08n_{C_5H_{12}}N_2 \\ n_{C_6H_{14}}C_6H_{14} + 9.5C_6H_{14}(O_2 + 3.76N_2) \rightarrow \\ 6n_{C_6H_{14}}CO_2 + 7n_{C_6H_{14}}H_2O + 35.72n_{C_6H_{14}}N_2 \end{gathered} \qquad (11)$$

Where n_{CH_4} , $n_{C_2H_6}$, $n_{C_3H_8}$, $\boldsymbol{n_{C_4H_{10}}}$, $n_{C_5H_{12}}$ and $n_{C_6H_{14}}$ are the mole fraction of CH_4, C_2H_6, C_3H_8, C_4H_{10}, C_5H_{12} and C_6H_{14} in the natural gas (0.8147, 0.1115,0.027, 0.0111, 0.0032, and 0.0003, respectively)
The amount of air needed to burn *1 kgmol* of natural gas is calculated as follows:

$$\begin{aligned} &(A/F)_{th} \\ &= 4.76\big(2n_{CH_4} + 3.5n_{C_2H_6} + 5n_{C_3H_8} + 6C_4H_{10} \\ &+ 8C_5H_{12}\ 9.5C_6H_{14}\big) \end{aligned} \qquad (12)$$

The actual amount of air required to burn 1 kg of natural gas is calculated as follows:

$$\begin{aligned} \lambda_{cc} &= \frac{(A/F)_{act}}{(A/F)_{th}} \\ (A/F)_{act} &= (A/F)_{th}\ \lambda_{cc} \end{aligned} \qquad (13)$$

Where:
λ_{cc}: is the excess air coefficient that is calculated by trial and error through the flowchart shown in Figure (4).

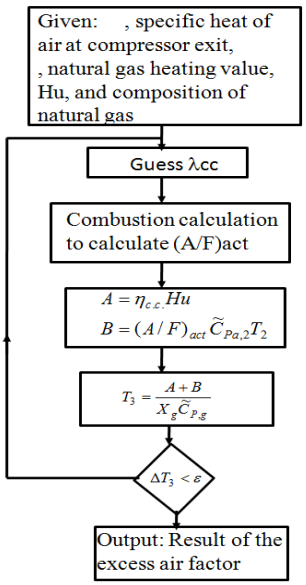

Figure 4: Flowchart for calculating the excess air coefficient for the combustion process inside the combustion chamber.

The mole fraction of combustion products per kilomole of natural gas is calculated as follows:

$$X_{CO_2} = n_{CH_4} + 2n_{C_2H_6} + 3n_{C_3H_8} + 4n_{C_4H_{10}} + 5n_{C_5H_{12}} + 6n_{C_6H_{14}} + n_{CO_2}\ ;\ kmol/kmol_{fuel} \qquad (14)$$

Where n_{CO_2} is the mole fraction of carbon dioxide present in natural gas.

$$X_{H_2O} = 2n_{CH_4} + 3n_{C_2H_6} + 4n_{C_3H_8} + 5n_{C_4H_{10}} + 6n_{C_5H_{12}} + 7n_{C_6H_{14}} + (n_{H_2O})_{air}(A/F)_{act}\ ;\ kmol/kmol_{fuel} \qquad (15)$$

Where $(n_{H_2O})_{air}$ is the mole fraction of water vapor present in the atmosphere:

$$X_{O_2} = (n_{O_2})_{air} + (\lambda_{cc} - 1)(A/F)_{act}\ ;\ kmol/kmol_{fuel} \qquad (16)$$

Where $(n_{O_2})_{air}$ is the mole fraction of oxygen present in moist atmospheric air.

$$X_{N_2} = (n_{N_2})_{air} + (A/F)_{act} + n_{N_2};\ kmol/kmol_{fuel} \qquad (17)$$

Where $(n_{N_2})_{air}$ is the mole fraction of nitrogen present in natural gas.
The number of moles of combustion products per kilomole of natural gas is calculated as follows:

$$X_g = X_{CO_2} + X_{H_2O} + X_{O_2} + X_{N_2} \qquad (18)$$

The mole fraction of each component of the combustion gases (i) per kilomole of combustion gases is calculated as follows:

$$Y_i = X_i/X_g\ ;\ \frac{kmol}{kmol_{combustion\ gases}} \qquad (19)$$

The molecular weight of combustion gases is calculated using the following equation:

$$M_g = \sum X_i M_i\ ;\ \frac{kmol}{kmol_{combustion\ gases}} \qquad (20)$$

The specific heat of combustion gases is calculated as follows:

$$\tilde{C}_{P,g} = \sum X_i \tilde{C}_{P,i}\ ;\ \frac{kmol}{kmol_{combustion\ gases}} \qquad (21)$$

The heat balance equation for the combustion process inside the combustion chamber is written as follows: The heat balance equation for the combustion process states that the rate of heat energy produced by burning the fuel plus the rate of heat energy of the air entering the combustion process and coming from the compressor equals the rate of heat energy of the combustion gases.

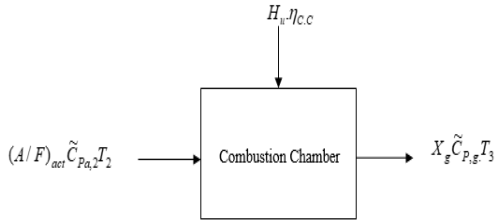

$$X_g\tilde{C}_{Pg}T_3 = \eta_{c.c.}H_u + (A/F)_{act}\,\tilde{C}_{Pa,2}\,T_2 \quad (22)$$

Where:

$\tilde{C}_{Pg}$,$\tilde{C}_{Pa}$: The specific heat of air and combustion gases can be calculated from the equations in the appendices.

X_g : The number of moles of combustion products per kilomole of natural gas.

Gas Turbine Calculations

The combustion gases enter the gas turbine at temperature T_3 and expand adiabatically with isotropic efficiency η_T, exiting the turbine at temperature T_4., T_4 is calculated using the following equations:

$$T_{4s} = T_3\left(\frac{1}{\pi_C}\right)^{(\gamma_g-1)/\gamma_g} \quad (23)$$

$$T_4 = T_3 + (T_{4s} - T_3).\eta_T \quad (24)$$

Where:

γ_g is the isentropic exponent of air ($\gamma g = \widetilde{C}_{P,g} / \widetilde{C}_{v,g}$)

η_T is the isentropic efficiency of the turbine.

$\widetilde{C}_{P,g}$ is the specific heat of product gas at constant pressure (*kJ/ (kmol. K*))

$\widetilde{C}_{v,g}$ is the specific heat of product gas at constant volume (*kJ/ (kmol. K*))

The work produced by the gas turbine per mole of natural gas is calculated using the following equation

$$w_T = X_g\tilde{C}_{P,g}(T_2 - T_3).\eta_{mT};\ \frac{kJ}{kmol_{n.g.}} \quad (25)$$

Where η_{mT} mechanical efficiency of the turbine

The net electrical work produced by the gas plant per kilomole of natural gas is calculated as follows:

$$w_{N,GT} = \lfloor w_T + (A/F)_{act}\,.w_C\rfloor\eta_G;\ \frac{kJ}{kmol_{n.g.}} \quad (26)$$

Where η_G. is the efficiency of the electric generator.

The thermal efficiency of the gas station is calculated as follows:

$$\eta_{GT} = \frac{w_{N,GT}}{H_u} \quad (27)$$

Steam plant calculations

Referring to the steam station diagram in Figure (3), the steam station follows the following processes:

Heat addition process in a heat recovery boiler

The heat exchange process in the heat recovery boiler, as is clear from Figure (5), is expressed by the following equation, in reference to the symbols in Figure (5) [44-46].

$$Q_B = X_g\tilde{C}_{P,g}(T_4 - T_5) = X_s(h_{1s} - h_{11s}) \quad (28)$$

Where:

Q_B : is the total heat recovered in the heat recovery boiler (*kJ/kmolfuel*).

X_s : is the amount of steam generated in the heat recovery boiler per kilomole of natural gas (*kg/ kmol*$_{fue}$).

The temperature difference between the water and the exhaust gases at the pinch point (ΔT*pp*) is calculated in terms of the T-Q diagram in Figure (3) by calculating the temperature of the exhaust gases at the pinch point through the following equations:

$$X_g\tilde{C}_{P,g}(T_4 - T_{g,pp}) = X_s(h_{1s} - h_f(p_b)) \quad (29)$$

$$\Delta T_{pp} = T_{g,pp} - T_{sat} \quad (30)$$

Where: $T_{g,pp}$is the exhaust gas temperature at the pinch point.

T_{sat} is the saturation temperature at the boiler pressure.

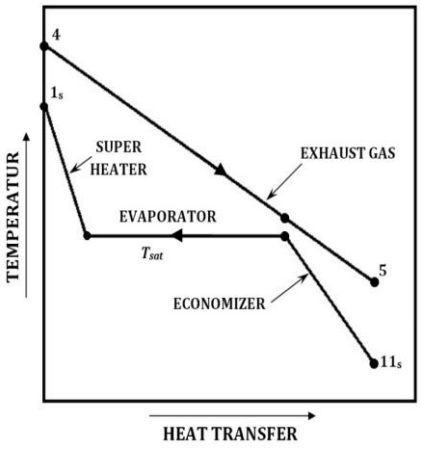

Figure 5: Temperature-heat exchange diagram of a heat recovery boiler

Heat exchange equation for the economizer

$$Q^{\circ}_{eco} = X_s[h_{f(PB)} - h_{11}] = X_g\tilde{C}_{P,g}(T_{g.pp} - T_5);kJ/kmol_{fuel} \quad (31)$$

Evaporator heat exchange equation

$$Q^{\circ}_{(evp+\sup)} = X_s[h_{1s} - h_{f(PB)}] = X_g\tilde{C}_{P,g}(T_4 - T_{g.pp})\ kJ/kmol_{fuel} \quad (32)$$

Expansion process in the turbine

The steam turbine work per kilomole of natural gas is calculated using the following equation:

$$w_{ST} = X_s[(h_{1s} - h_{2s}) + (1-\mu_1)(h_{2s} - h_{3s}) + (1-\mu_1-\mu_2)(h_{3s} - h_{4s}) + (1-\mu_1-\mu_2)(h_{5s} - h_{6s})\ ];\ kJ/kmol_{fuel} \quad (33)$$

Where:

μ_1 : The fraction of exhaust steam for the high-pressure surface heater.

μ_2: The fraction of exhaust steam for the open deaerator.

μ_3 : The fraction of exhaust steam for the low-pressure surface heater.

$\mu_1, \mu_2, \mu_3$are calculated during the thermal equilibrium of the heaters as follows:

Thermal equilibrium of a high-pressure surface heater

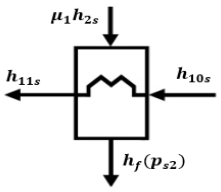

$$\mu_1[h_{2s} -] = h_{11s} - h_{10s} \quad (34)$$

Where

$$h_{10s} = h_f(p_{s3}) + w_{F.P} \quad (35)$$

Where $w_{F.P}$ the work of the boiler feed pump is calculated using the following equation:

$$w_{F.P} = \frac{p_{s1} - p_{s3}}{\rho_w\,\eta_P} \quad (36)$$

Where ρ_w is the density of water, η_P is the pluripotent efficiency of the pump.

Thermal equilibrium of the open heater (deaerator)

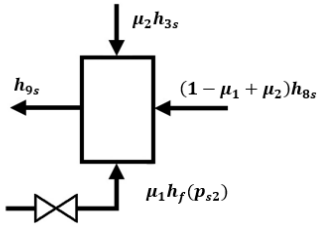

$$\mu_2 h_{3s} + (1-\mu_1+\mu_2)h_{8s} + \mu_1 h_f(p_{s2}) = h_{9s} \quad (37)$$

Where:

$$h_{8s} = h_f(p_{s4}) \quad (38)$$

$$h_{9s} = h_f(p_{s3}) \quad (39)$$

Thermal equilibrium of a low-pressure surface heater

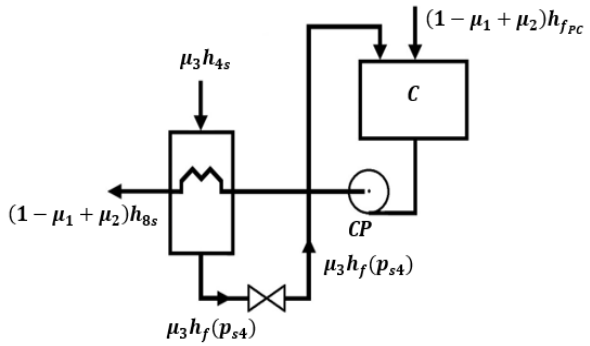

$$\mu_3 h_{4s} + (1-\mu_1+\mu_2-\mu_3)h_f(p_c) + w_{CP} = (1-\mu_1+\mu_2)h_{8s} \quad (40)$$

Where w_{CP} is the work of the condensation pump per kg of steam generated from the boiler, which is calculated using the following equation:

$$w_{C.P} = (1-\mu_1+\mu_2)\frac{p_{s3}-p_c}{p_w \eta_P} \quad (41)$$

Where p_c is the condenser pressure.

Special equations for combined gas/steam power plant

The goal of any combined gas/steam power plant is to increase the thermal efficiency value [44-46].

The total work produced by the combined gas/steam power plant is the sum of the work produced by the gas power plant and the work produced by the steam power plant:

$$w_{comb} = w_{GT} + w_{ST} \; ; \; \frac{kJ}{kmol_{fuel}} \quad (42)$$

The overall thermal efficiency of the combined gas/steam power plant is calculated as follows:

$$\eta_{comb} = \frac{w_{comb}}{H_u} \quad (43)$$

Figure (6) shows the flowchart of the computer program used in the calculations for the combined gas/steam power plant, which is based on the ees language.

Results and discussion

The Both a basic gas power plant with a combustion chamber, air compressor, and gas turbine, as well as a steam power plant with specifications similar to one of the units of the Derna steam power plant, are included in the proposals for the combined gas/steam power plant. In the Derna steam power plant, the conventional combustion boiler is replaced with a heat recovery boiler that uses the gas turbine's combustion gases as a heat source for the heat recovery system. boiler to generate steam that meets the same specifications as those of the Derna steam power plant boiler, which are 87 bar and 520°C. The steam turbine is the same as the one used in the Derna steam plant's four expansion stages. In order to heat the feedwater for the heat recovery boiler, steam is released in between the turbine stages, as shown in Figure 3. After the initial expansion stage, the steam is expelled at a pressure of 21.8 bar, which heats the feedwater in the high-pressure superheater. After the second expansion stage, the steam is released from the turbine at a pressure of 6.02 bar to heat the feedwater through the open deaerator. After the third expansion stage, the steam is released from the steam turbine at a pressure of 1.15 bar to heat the feedwater through the low-pressure superheater. Condensed and released steam from the high-pressure superheater can return to the rear and enter the open deaerator through an expansion valve. Figure 3 shows the evacuated low-pressure superheater.

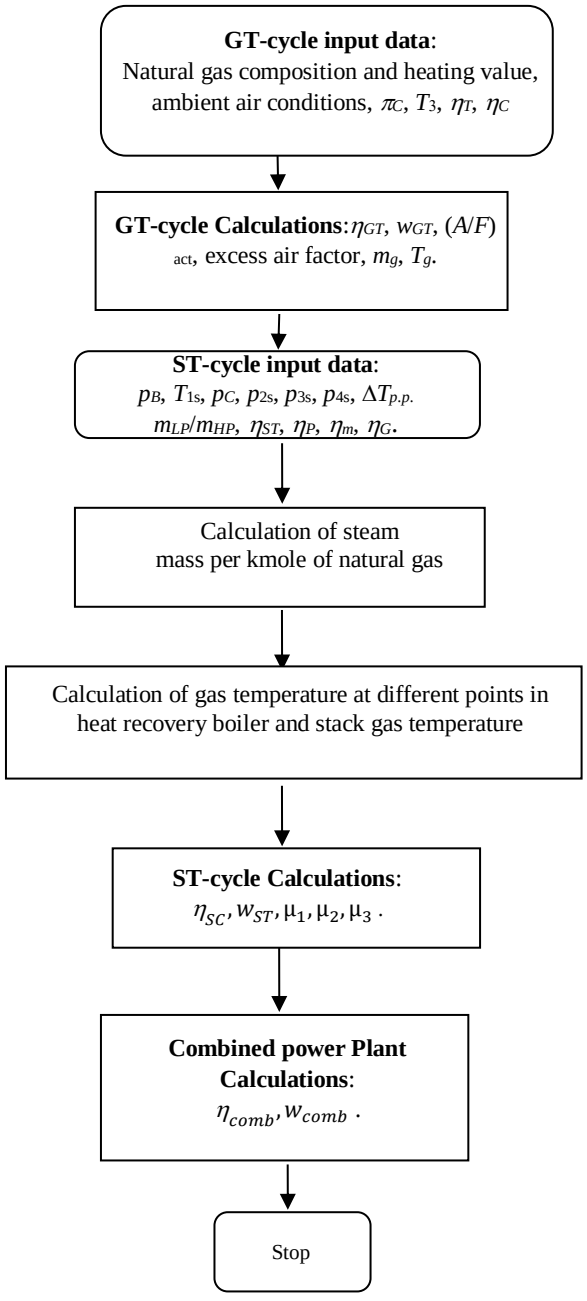

Figure 6: Flowchart of the joint station accounting program

Effect of the pressure ratio π_C of the compressor and the temperature T_3 at the gas turbine inlet on the efficiency of the gas cycle

The efficiency of the gas cycle is influenced by the compressor pressure ratio π_C and the temperature of the combustion gases leaving the combustion chamber and entering the turbine T3, as shown in Figure 7.

The graph indicates that for any value of π_C, the value of gas cycle efficiency increases in tandem with T3. Additionally,

we can see from the figure that the gas cycle efficiency rises for each value of T3 until it reaches its maximum, after which it falls as the value of π_C grows. It is also observed that when T3 grows, the value of π_C, at which the gas cycle's maximum efficiency rises increases. This leads us to the conclusion that in order to have a high gas cycle efficiency, T3 must rise to the greatest value feasible and π_C must be at a certain value that corresponds to T3, which provides the gas cycle's maximum efficiency.

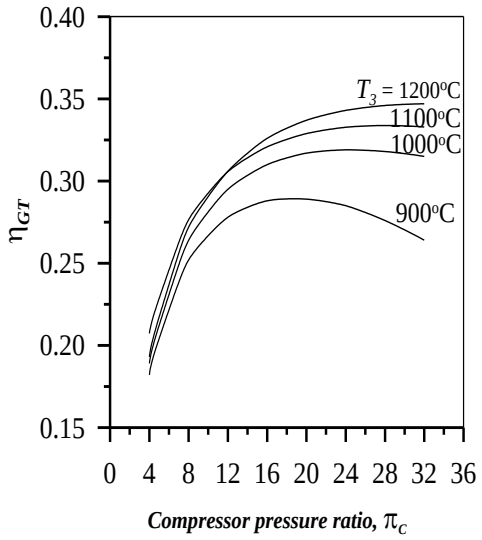

Figure 7: The impact of both and T3 on the gas station's efficiency

Effect of pressure ratio π_C and temperature T_3 on gas turbine outlet temperature T_4

The temperature change of the gases leaving the gas turbine as both π_C and T3 vary is seen in Figure 9. As can be seen from Figure (8), it is well known that the temperature of the gases leaving the gas turbine drops as the pressure ratio of the gas turbine increases to equal the compressor's pressure ratio, ignoring the pressure losses in the combustion chamber and the pressure differential from the atmospheric pressure at the gas turbine's exit. Figure (8) makes it evident that when the temperature of the gases entering the gas turbine rises at all **values, the temperature of the gases leaving the gas turbine also rises. It is observed that the highest The efficiency of the

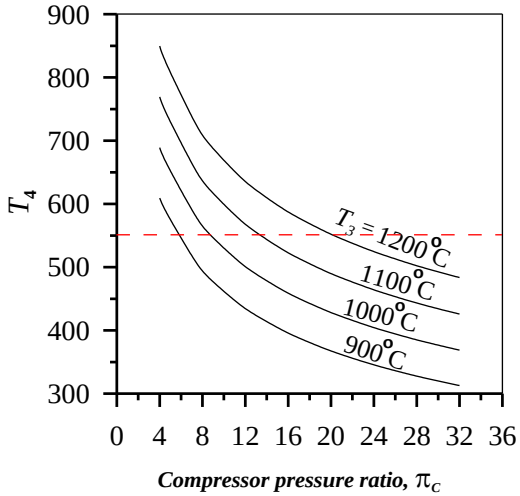

Figure 8: The effect of both π_C& T_3 on the temperature exiting the gas turbine T_4

gas cycle at T3 = 900oC is 0.268 at $\pi_C = 12$ and, the maximum efficiency of the gas cycle at T3 = 1000oC is 0.292 at $\pi_C = 16$, , and the maximum efficiency of the gas cycle at T3 = 1100oC is 0.314 at $\pi_C = 24$, and the maximum efficiency of the gas cycle at T3 = 1200oC is 0.334 at $\pi_C = 28$, The temperature of the gases leaving the gas turbine must be higher than the temperature of the steam produced by the heat recovery boiler because the gases leaving the gas turbine are the heat source that creates steam in the boiler.

The temperature of the gases leaving the gas turbine must not be lower than 520 °C since the steam produced by the heat recovery boiler has a temperature of 520 °C. The dotted line in Figure 9 indicates that the temperature of the gases leaving the gas turbine must not be lower than 550 °C, assuming that there is a minimum difference of 30 °C between the temperature of the gases leaving the gas turbine and the steam produced by the heat recovery boiler. From the figure, we conclude that if T3 = 900oC, the value π_C must not exceed 6. If T3 = 1000oC, the value π_C must not exceed 10. If T3 = 1100oC, the value π_C must not exceed 14. If T3 = 1200oC, the value $\pi_C$must not exceed 20.

Efficiency of gas cycle & steam cycle & combined cycle

The efficiency change of each gas cycle, steam cycle, and combination cycle station is depicted in Figure 9 at a gas turbine inlet temperature T3=1200oC and with the compressor's pressure ratio restrictions permitted for the combined cycle operation. Because the statistics from the steam cycle are constant, we may conclude that the thermal efficiency of the steam cycle remains constant despite changes in the compressor's pressure ratio, but the gas cycle's efficiency does not. rises steadily as the compressor's pressure ratio rises, and the combined cycle station's efficiency rises as well, peaking at 0.4724 at a compressor pressure ratio $\pi_C = 12$ before slightly declining as the compressor's pressure ratio rises.

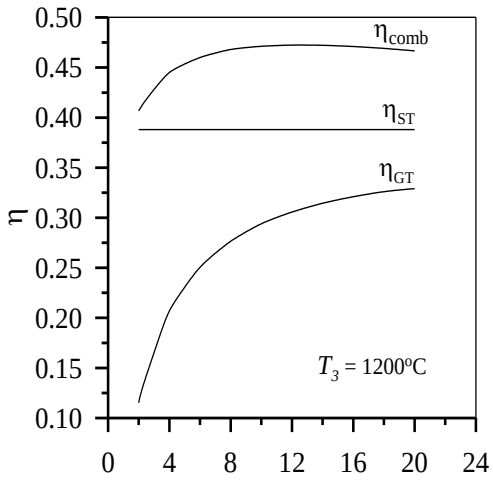

Figure 9: Change in efficiency of the gas, steam, and combined cycle with the pressure ratio of the compressor

Gas & Steam Power Plant & Combined Plant Capacity

With a gas turbine inlet temperature of T3 = 1200oC, Figure 10 illustrates how the power of each gas cycle, steam cycle, and combined cycle power plant varies in response to variations in the compressor pressure ratio. The gas cycle power stays constant at 65 MW, which is the same design power as one of the units at the Derna steam plant, because the combined cycle power design in this study is based on the combined cycle power producing the same design power as one of the units at the Derna steam plant. Figure (10) makes it evident that when the compressor pressure ratio rises, the gas

cycle power and combined cycle power, which equals the total of the gas cycle and steam cycle powers, continue to rise. At the highest efficiency of the combined cycle power plant, the gas cycle's electrical power value $\pi_C = 12$ is 119.215 MW.

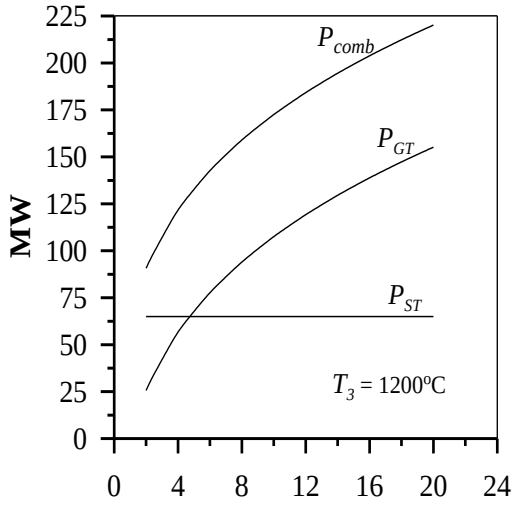

Figure 10: Change in the capacity of the gas cycle, steam, and combined cycle with the pressure ratio of the compressor

Natural gas mass ratio and air ratio required increase

As the compressor pressure ratio changes, Figure 11 illustrates how the natural gas mass ratio and the extra air ratio both vary. It is observed that when the compressor pressure ratio rises, the surplus air ratio λ the ratio of the actual air mass to the theoretical air mass needed to burn the combustible components of natural gas, increases by a small percentage. This is because the temperature of the air exiting the compressor and entering the combustion chamber rises as the compressor pressure ratio does. The value of λ rises as the compressor pressure ratio rises because the temperature of the gases produced by combustion is constant at T3 = 1200oC.

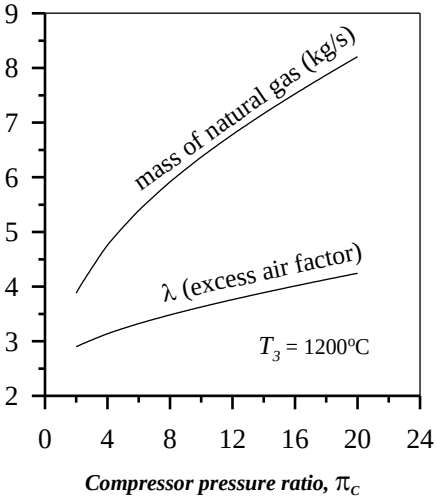

Figure 11: Change in the percentage of excess air and the required natural gas rate with the pressure ratio of the compressor

Figure (11) shows that when the compressor pressure ratio rises, the mass rate of natural gas needed for combustion rises noticeably. The reason for this is that when the compressor pressure ratio increases, the temperature of the gases leaving the gas turbine, the heat source for the heat recovery boiler, decreases, and the temperature rate needed for the heat recovery boiler remains constant. The steam cycle capacity and its parameters are fixed and are the same as those of the Derna steam station.

Air mass ratio and combustion gases

At the gas turbine inlet temperature T3 = 1200oC, Figure (12) illustrates how the change in compressor pressure ratio value affects the rate of combustion gases produced by the combustion process as well as the rate of air mass required for the combustion process. The higher the compressor pressure ratio value, the higher the mass rate of the air leaving the compressor and the mass rate of the combustion gases produced by the fire. The reason for this is that as the compressor pressure ratio value changes, the heat rate needed by the heat recovery boiler stays constant. This is because changes in the compressor pressure ratio have no effect on the steam cycle data or the electricity produced by the steam plant. The temperature of the gases leaving the gas turbine and entering the heat recovery boiler drops as the compressor pressure ratio rises. In order to make up for the drop in temperature of the gases leaving the gas turbine, the mass rate of the air entering the combustion process as well as the natural gas needed for the combustion process, both rise.

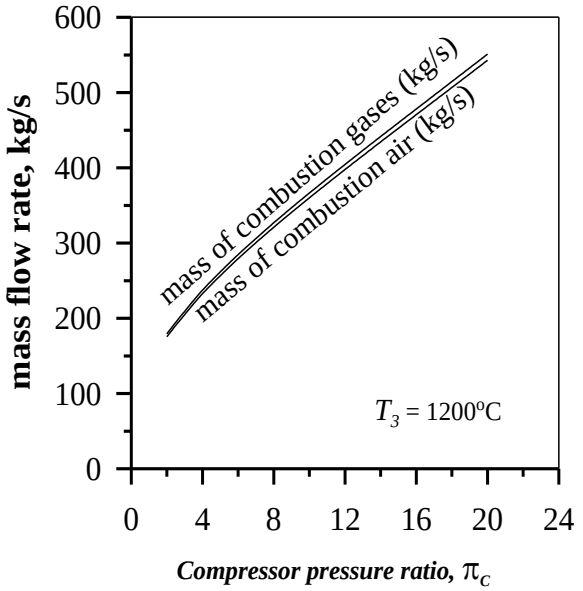

Figure 12: Change in the mass rate of air and combustion gases with the pressure ratio of the compressor

Temperature of exhaust gases exiting the chimney

As the compressor pressure ratio changes, Figure (13) illustrates how the temperature of the exhaust gases leaving the chimney changes. Assuming a temperature differential of 15°C at the pinch point—the temperature of the gases entering the economizer section of the heat recovery boiler—the temperature of the combustion gases at the pinch point is 315.9°C because the heat recovery boiler has a single pressure of 87 bar, which translates to a saturation (boiling) temperature of 300.9°C. Figure (13) illustrates how the mass rate of the exhaust gases rises as the compressor's pressure ratio increases. Due to the unaltered parameters of the steam cycle, the temperature of the exhaust gases leaving the chimney rises to correspond with the increase in the mass rate of the combustion gases as the compressor pressure ratio rises. This is because the temperature needed for the economizer remains constant.

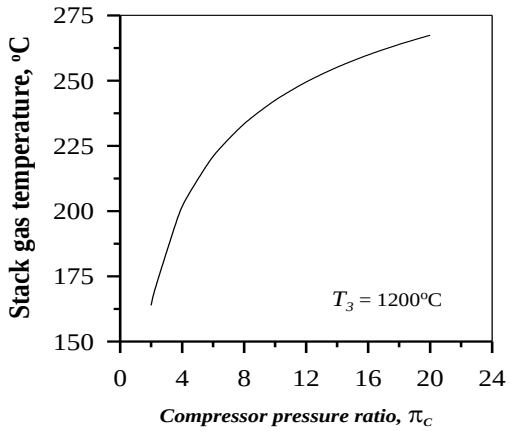

Figure 13: Change in the temperature of the exhaust gases coming out of the chimney with the pressure ratio of the compressor

Conclusions

The aim of this research is to determine if it is feasible to convert a 65 MW unit of the Derna steam power plant into a combined gas/steam power plant with the same design parameters and a steam cycle that generates the same amount of power as the Derna steam power plant. It was evident from the theoretical computations' outcomes that:

For the combined plant to function with the steam cycle characteristics for every value of the T3 temperature at the gas turbine inlet, the pressure ratio of the gas cycle compressor must be limited.(if T3 = 900°C, the value of π_C should not exceed 6; if T3 = 1000°C, the value of π_C should not exceed 10; if T3 = 1100°C, the value of π_C should not exceed 14; and if T3 = 1200°C, the value of π_C should not exceed 20).

Since the steam cycle parameters are fixed at T3 = 1200°C, we discover that the steam cycle's thermal efficiency stays constant and is unaffected by variations in the compressor pressure ratio. Nonetheless, when the compressor pressure ratio rises, the gas cycle's efficiency keeps improving. As the compressor pressure ratio rises, the combined cycle's efficiency improves as well, peaking at 47.24% at π_C = 12. After that, it somewhat drops as the compressor pressure ratio rises.

The electrical power produced by the gas cycle is 119.215 MW at T3 = 1200°C, and the electrical power produced by the combined cycle is 184.215 MW at the maximum efficiency of the combined cycle.

The mass ratio of the air leaving the compressor, the natural gas needed for combustion, and the gases generated during combustion all rise when the compressor pressure ratio is raised. Additionally, the air-excess coefficient rises.

The temperature of the exhaust gases leaving the chimney rises as the compressor pressure ratio is increased, which accelerates the pace at which the exhaust gases lose heat.

With a maximum thermal efficiency of 47.24%, a combined gas/steam power plant that produces 65 MW of electrical power and consists of a steam power plant that meets the same specifications as one of the units of the Derna steam power plant needs a gas turbine cycle with a compressor pressure ratio of 12, an air mass rate of 397.75 kg/s going through the compressor, an electrical power output from the gas cycle of 119.215 MW, and a flue gas temperature of 249.5°C.

The exhaust gases squander a lot of heat since, in this study, the minimum temperature of the exhaust gases leaving the chimney is at least 164°C. This is due to the single-pressure nature of the heat recovery boiler that was employed in this investigation. As a result, research on a combined gas/steam plant with a dual-pressure or triple-pressure heat recovery boiler is advised.

Given that every steam cycle parameter was determined in this study, it is advised to investigate how these parameters affect the combined plant's performance.

An economic feasibility study is recommended for the project to assess the financial viability of converting the station, including implementation costs, fuel savings, and payback period.

Author Contributions: Ahmed: Conceptualization, methodology; Shahat, Fouzi, Rabae, Abdul-Hakim and: writing—original draft preparation; Tarek, Yasser and Ibrahim: review and editing. All authors have read and agreed to the published version of the manuscript."

Funding: "This research received no external funding."

Data Availability Statement: "The data are available at request OR Not applicable."

Acknowledgments: "The authors would like to express their appreciation to the Research Center for Renewable Energy and Sustainable Development, Wadi Alshatti University, Brack-Libya."

Conflicts of Interest: "The authors declare no conflict of interest."

References

[1] H. El-Khozondar, et al. "Feasibility of Concentrating Solar Power as a Solar Fuel for Electrical Power Stations: A Case Study of Ubari Gas-Power Station in Libya." *Wadi Alshatti University Journal of Pure and Applied Sciences*, vol. 4, no. 1, pp, 56-69, 2026. https://doi.org/10.63318/ waujpasv4i1_06

[2] S .Abdulwahab, et al. "Meeting Solar Energy Demands: Significance of Transposition Models for Solar Irradiance." *ijees*, vol. 1, no. 3, pp. 90–105, 2023. https://doi.org/10.65998/ijees.v1i3.52

[3] A. Youssef. "Nuclear Plants Trends for Development Planning in Egypt," *Wadi Alshatti University Journal of Pure and Applied Sciences*, vol. 4, no,1, pp. 277–286, 2026.: https://doi.org/10.63318/waujpasv4i1_29.

[4] N. Fathi, et al. "Technical and environmental cost-benefit analysis of strategies towards a green economy in the electricity sector in Libya." *Economics and Policy of Energy and the Environment*, vol. 2, pp. 133-167, 2025. https://doi.org/ 10.3280/EFE2025-002007

[5] N. Fathi, M. Irhouma, and M. Salem. "Towards Green Economy: : Case of Electricity Generation Sector in Libya." *Solar Energy and Sustainable Development Journal*, vol. 14, no. 1, pp. 334–360, 2025. https://doi.org/10.51646/ jsesd.v14i1.549

[6] Y. Nassar, K. Aissa, and S Alsadi. "Estimation of Environmental Damage Costs from CO2e Emissions in Libya and the Revenue from Carbon Tax Implementation." *Low Carbon Economy*, vol. 8, pp. 118-132, 2017. https://doi.org/10.4236/lce.2017.84010

[7] A .Makhzom, et al. "Estimation of CO2 emission factor for Power Industry Sector in Libya." *The 8th International Engineering Conference on Renewable Energy and Sustainability,* 08-09 May 2023, Gaza, Palestine. https://doi.org/10.1109/ieCRES57315.2023.10209528

[8] A. Elmabruk, M. Salem, M. Khaleel, and A. Mansour. "Prediction of Wind Energy Potential in Tajoura and Mislata Cities." *Wadi Alshatti University Journal of Pure and Applied Sciences*, vol. 3, no. 2, pp. 125-131, 2025. https://doi.org/10.63318/waujpasv3i2_17

[9] A. ElNoaman, et al. "Evaluation of the underground soil thermal storage properties in Libya." *Renewable energy*, vol.

31, no. 5, pp. 593-598, 2006. https://doi.org/10.1016/j.renene.2005.08.001

[10] I. Imbayah, et al. "Modeling A 600 MW Floating Photovoltaic System in Al-Khums city, Libya: Performance Analysis and Implementation Using PVSyst." *Wadi Alshatti University Journal of Pure and Applied Sciences*, vol. 4, no. 1, pp. 223-237, 2026. https://doi.org/10.63318/waujpasv4i1_24

[11] M. Ameri, and P. Ahmadi. "Exergy analysis of a 420 MW combined cycle power plant", International journal of energy research 2007, https://doi.org/10.1002/er.1351

[12] A. Abusoglu, and M. Kanoglu. "Exergoeconomic analysis and optimization of combined heat and power production: A review." *Renewable and Sustainable Energy Reviews*, 2009. https://doi.org/10.1016/j.rser.2009.05.004

[13] O. Balli, H. Aras, Energetic and exergetic performance evaluation of a combined heat and power system with the micro gas turbine (MGTCHP). *Int J Energy Res.,* vol. 31, p. 1425e1440, 2007. https://doi.org/ 10.1002/er.1308

[14] M. Mohammed, Y. Hamad, M. Hamdan, and Y. Nassar, "Energy and Exergy Analysis of an Al-Hussein Steam Power Plant in Jordan Using Engineering Equation Solver (EES)." *Wadi Alshatti University Journal of Pure and Applied Sciences*, vol. 4, no. 1, pp. 199–209, 2026, https://doi.org/10.63318/waujpasv4i1_21.

[15] A. Kaviri, M. Jaafar, and T. Lazim. "Modeling and multi-objective exergy based optimization of a combined cycle power plant using a genetic algorithm." *Energy conversion and management*, vol. 58, pp. 94-103, 2012, https://doi.org/10.1016/j.enconman.2012.01.002

[16] M. Abdalla *et al.*, "Performance and Efficiency of Combined Cycle Power Plants." 2022. https://docs.lib.purdue.edu/cgi/viewcontent.cgi?article=3272&context=iracc

[17] M. Mohammed, E. Mohammed, R. Elzer, and Y. Nassar, "Techno-Economic Feasibility of Parabolic Trough Solar Steam for Thermal Enhanced Oil Recovery." *Wadi Alshatti University Journal of Pure and Applied Sciences*, vol. 4, no. 1, pp. 184–190, 2026. https://doi.org/10.63318/waujpasv4i1_19.

[18] M. Abdalla, S. Pannir, A. Ahmed, A. Mahjob, and S. Abdalla, "Regenerative Gas Turbine Power Plant: Performance & Evaluation." *Purdue e-Pubs*, 2021. https://docs.lib.purdue.edu/icec/2694/

[19] E. Lowe, *et al.*, *Hydrobiologia*, vol. 448, no. 1/3, pp. 11–18, 2001, https://doi.org/10.1023/a:1017541010768.

[20] A. Grandemange, R. Lasseur, C. Sauvageon, E. Benoit, and P. Berny., "Distribution of VKORC1 single nucleotide polymorphism in wild *Rattus norvegicus* in France." *Pest Management Science*, vol. 66, no. 3, pp. 270–276, 2009. https://doi.org/10.1002/ps.1869.

[21] R. Quy, G. Massei, M. Lambert, J. Coats, L. Miller, and D. Cowan. "Effects of a GnRH vaccine on the movement and activity of free-living wild boar (Sus scrofa)." *Wildlife Research*, vol. 41, no. 3, pp. 185–185, 2014. https://doi.org/10.1071/wr14035.

[22] H. Susanto, K. Abdullah, A. Uyun, S. Nur, and T. Mahlia. "Turbine Design for Low Heat Organic Rankine Cycle Power Generation using Renewable Energy Sources." *MATEC Web of Conferences*, vol. 164, p. 01012, 2018. https://doi.org/10.1051/matecconf/201816401012.

[23] S. Moneim, and R. Ali. "Performance evaluation of heat transfer enhancement for internal flow based on exergy analysis." *International Journal of Exergy*, vol. 4, no. 4, p. 401, 2007. https://doi.org/10.1504/ijex.2007.015081.

[24] N. Hasan, J. Rai, and B. Arora. "Optimization of CCGT power plant and performance analysis using MATLAB/Simulink with actual operational data." *SpringerPlus*, vol. 3, no. 1, p. 275, 2014. https://doi.org/10.1186/2193-1801-3-275.

[25] R. Venkatesh, and W. Christraj. "Performance Analysis of Solar Water Heater in Multipurpose Solar Heating System." *Applied Mechanics and Materials*, vol. 592–594, pp. 1706–1713, 2014. https://doi.org/10.4028/www.scientific.net/amm.592-594.1706.

[26] E. Ogbonnaya, H. Ugwu, and E. Diema. "A model-based mixed data approach for optimizing the performance of an offshore gas turbine compressor." *Journal of Vibration and Wave Propagation*, 2013. https://doi.org/10.7726/jvwp.2013.1001.

[27] A. Tiwari, M. Hasan, and M. Islam. "Exergy Analysis of Combined Cycle Power Plant: NTPC Dadri, India." *International Journal of Thermodynamics*, vol. 16, no. 1, 2012. https://doi.org/10.5541/ijot.443.

[28] M. Jefferson, P. Zhou, and G. Hindmarch. "Analysis by computer simulation of a combined gas turbine and steam turbine (COGAS) system for marine propulsion." *Journal of marine engineering and technology*, vol. 2, no. 1, pp. 43–53, 2003. https://doi.org/10.1080/20464177.2003.11020164.

[29] M. Dzida, and W. Olszewski. "Comparing combined gas tubrine/steam turbine and marine low speed piston engine/steam turbine systems in naval applications." *Polish Maritime Research*, vol. 18, no. 4, pp. 43–48, 2011. https://doi.org/10.2478/v10012-011-0025-8.

[30] F. Zhou, and J. Huang, "Cybersecurity data breaches and internal control." *International Review of Financial Analysis*, vol. 93, p. 103174, 2024. https://doi.org/10.1016/j.irfa.2024.103174

[31] R. Quy, G. Massei, M. Lambert, J. Coats, L. Miller, and D. Cowan. "Effects of a GnRH vaccine on the movement and activity of free-living wild boar (Sus scrofa)." *Wildlife Research*, vol. 41, no. 3, pp. 185–185, 2014. https://doi.org/10.1071/wr14035.

[32] A. Abioye, et al. "Model based predictive control strategy for water saving drip irrigation." *Smart Agricultural Technology*, vol. 4, p. 100179, 2023. https://doi.org/10.1016/j.atech.2023.100179.

[33] A. Bois, M. Boix, O. Therond, L. Montastruc, J. Villerd, and I. Touche. "Multi-actor approach to manage the water-energy-food nexus at territory scale." *Computers & Chemical Engineering*, vol. 189, pp. 108773–108773, 2024. https://doi.org/10.1016/j.compchemeng.2024.108773.

[34] I. Mangir, M. Salem, A. Otman, Y. Nassar. "The impact of fuel type on the economic, environmental, and energy performance of power generation plants: A case study of the Ubari gas power plant." *Wadi Alshatti University Journal of Pure and Applied Sciences*, vol. 4, no. 2, p. 59, 2026. https://doi.org/10.63318/waujpasv4i2_08.

[35] T. Hanlin, and C. Aske. "Gerold Spath und die Rapperswiler Texte." *German Studies Review*, vol. 26, no. 2, p. 469, 2003. https://doi.org/10.2307/1433404.

[36] C. Firth, et al. "Detection of Zoonotic Pathogens and Characterization of Novel Viruses Carried by Commensal Rattus norvegicus in New York City." *mBio*, vol. 5, no. 5, 2014. https://doi.org/10.1128/mbio.01933-14.

[37] V. Cenusa, M. Feidt, R. Benelmir, and A. Badea. "Optimisation des cycles combinés gaz/vapeur avec un ou deux niveaux de pression et chaudière à surface d'échange impose." *Oil & Gas Science and Technology*, vol. 61, no. 2, pp. 225–235, 2006. https://doi.org/10.2516/ogst:2006016x.

[38] B. Vahidi, M. Tavakoli, and W. Gawlik. "Determining Parameters of Turbine's Model Using Heat Balance Data of Steam Power Unit for Educational Purposes." *IEEE Transactions on Power Systems*, vol. 22, no. 4, pp. 1547–1553, 2007. https://doi.org/10.1109/tpwrs.2007.907509.

[39] M. Hashmi, T. Lemma, S. Ahsan, and S. Rahman. "Transient Behavior in Variable Geometry Industrial Gas Turbines: A Comprehensive Overview of Pertinent Modeling Techniques," *Entropy*, vol. 23, no. 2, p. 250, 2021. https://doi.org/10.3390/e23020250.

[40] F. Jurado, A. Cano, and J. Carpio. "Modelling of combined cycle power plants using biomass." *Renewable Energy*, vol. 28, no. 5, pp. 743–753, 2003. https://doi.org/10.1016/s0960-1481(02)00113-1.

[41] E. Martelli, F. Alobaid, and C. Elsido. "Design Optimization and Dynamic Simulation of Steam Cycle Power Plants: A Review." vol. 9, 2021. https://doi.org/10.3389/fenrg.2021.676969.

[42] N. Babu, S. Bhagat, L. Saikia, T. Chiranjeevi, R. Devarapalli, and F. Márquez. "A Comprehensive Review of Recent Strategies on Automatic Generation Control/Load Frequency Control in Power Systems." *Archives of Computational Methods in Engineering*, 2022. https://doi.org/10.1007/s11831-022-09810-y.

[43] R. Khalili, H. Rabieyan, A. Khodadadi, B. Zaker, M. Karrari, and S. Karrar. "Mathematical Modelling and Parameter Estimation of an Industrial Steam Turbine-Generator Based on Operational Data," *IFAC-PapersOnLine*, vol. 51, no. 2, pp. 214–219, 2018. https://doi.org/10.1016/j.ifacol.2018.03.037.

[44] D. Trivedi, R. Bagga, and J. Chokshi, "Structural Engineering Challenges in Structures for Cooling Water System in Thermal Power Plant." *Procedia Engineering*, vol. 51, pp. 141–150, 2013. https://doi.org/10.1016/j.proeng.2013.01.021.

[45] M. Borgnakke, H. Moran, D. Shapiro, D. Boettner, and M. Bailey. *Fundamentals of Engineering Thermodynamics.* John Wiley & Sons Canada, Limited, 2010.

[46] Y. Kim, C. Borgnakke, and R. E. Sonntag, "Equation of state for 1,1-difluoroethane (R152a)." *International Journal of Energy Research*, vol. 21, no. 7, pp. 575–589, 1997> https://doi.org/10.1002/(sici)1099-114x(19970610)21:7%3C575::aid-er272%3E3.0.co;2-f

.

Appendix

Table A1: The composition, molecular weight, and heating value of natural gas

No.	Component's name	Mole fraction, %
1	Nitrogen, N_2	0.52
2	Carbon Dioxide, CO_2	2.7
3	Hydrogen Sulphide	N/D
4	Methane, CH_4	81.47
5	Ethane, C_2H_6	11.15
6	Propane, C_3H_8	2.7
7	iso-Butane, C_4H_{10}	0.5
8	n-Butane, C_4H_{10}	0.61
9	iso-Pentane, C_5H_{12}	0.19
10	n-Pentane, C_5H_{12}	0.13
11	Hexane, C_6H_{14}	0.03
12	Total	100
13	Molecular weight	19.848 kg/kmol
14	Heating value, Hu	1,141.15 MJ/kmol

Table A2: Input Data for the considere combined gas/steam power plant

No.	Parameter	Value
1	Ambient air conditions	25°C, 1 bar, 60% relative humidity
2	Live steam conditions	87 bar, 550 °C, 66.815 kg/s
3	Pressure of extracted steam for HP feed water heater	21.8 bar
4	Deaerator pressure	6.02 bar
5	Pressure of extracted steam for HP feed water heater	1.15bar
6	Conditions pressure	0.062 bar
7	Steam turbine adiabatic efficiency, η_T	85%
8	Pump polytropic efficiency, η_P	75%
9	Mechanical efficiency, η_m	97%
10	Generator efficiency, η_G	98%
11	Boiler efficiency, η_c	98.5%
12	Compressor pressure ratio	4-36
31	GT-inlet temperature	900-1200°C
41	Compressor adiabatic efficiency	89%
51	GT-adiabatic efficiency	89%
61	Temperature difference ($T_4 - T_{1s}$)	45°C
17	Temperature difference at pinch point	15°C
81	Pump adiabatic efficiency	75%
91	Mechanical efficiency	98%
20	Generator efficiency	99%
21	Stack gas temperature	125°C
22	Air mass flow rate	150 kg/s